Recent Investigations of Cascaded GEM and MHSP Detectors

R. Chechik, A. Breskin, G. P. Guedes, D. Mörmann, J. M. Maia, V. Dangendorf, D. Vartsky, J. M. F. Dos Santos, and J. F. C. A. Veloso

***Abstract*—We present results from our recent investigations on detectors comprising cascaded gas electron multipliers (GEMs) and cascaded GEMs with microhole and strip plate (MHSP) multiplier as a final amplification stage. We discuss the factors governing the operation of these fast radiation-imaging detectors, which have single-electron sensitivity. The issue of ion-backflow and ion-induced secondary effects is discussed in some detail, presenting ways for its suppression. Applications are presented in the fields of photon imaging in the ultraviolet-to-visible spectral range as well as X-ray and neutron imaging.**

***Index Terms*—Gas electron multiplier (GEM), gaseous photon detectors, ion feedback, radiation imaging detectors.**

I. Introduction

THE gas electron multiplier (GEM) [1] presents attractive features, making it an amplifying-element of choice in a variety of radiation imaging detectors [2]. It is fast, robust, and can be produced with a relatively large area (30 cm × 30 cm). The GEM collects and multiplies charges induced by radiation either in a gas volume or on a solid radiation converter. The multiplied charges are collected onto a patterned anode, to provide high-resolution localization. According to the size of the initially deposited charge, the GEM can be employed as a stand-alone multiplier or in a cascaded mode. The optical opacity of the electrode and the confinement of the avalanche to the holes result in highly suppressed photon-mediated and photon-induced processes. Thus, high charge gain, of typically 10^3–10^4, is achieved with a single GEM in common counting gases [3]. Cascaded triple- and quadruple-GEMs attain gains of about 10^5–10^6 in various Ar-based noble gas mixtures [4] and higher gains in Ar-CH_4 and in pure CF_4 [5]. Multi-GEM detectors guarantee stable operation in charged-particles [6] and X-ray [7] detection, and high sensitivity to single charges; the latter is the basis for multi-GEM gaseous photomultipliers [4], [8]. They are investigated and applied for particle tracking [9], as imaging elements in time projection chambers (TPCs) [10], for X-ray [11], [12] and thermal-neutron imaging [13], [14], and for the imaging of ultraviolet (UV) photons [15] and visible light [16], [8].

In this paper we explain some processes governing the operation of radiation detectors based on multi-GEMs and multi-GEMs followed by the novel microhole and strip (MHSP) multiplier [17], [18]. We present our recent results on ion backflow and its reduction or suppression in both cascaded multipliers. Applications to X-ray, neutron, and photon imaging are presented.

II. Electron Transport in Cascaded-GEM Detectors—A Concise Recall

The coupling of cascaded-GEMs to gaseous converters is straightforward, and the efficiency of electron focusing into the first-GEM holes has been thoroughly studied [19]. It was established that full detection efficiency for charges deposited above the GEM is obtained with small field $\mathrm{E_{drift}}$ in the conversion region, of the order of 100–500 V/cm at atmospheric pressure.

The coupling of GEM to a solid converter may be done in two modes. The first is the *semitransparent mode*, in which the converter is placed at some distance above the first GEM, with a field $\mathrm{E_{drift}}$ between them. The second is the *reflective mode* (Fig. 1), in which the converter is deposited on top of the first GEM, and a field $\mathrm{E_{drift}}$ is defined in the gap above it, by a mesh electrode. In many cases the reflective mode is preferable, permitting the use of a thick converter with high conversion efficiency.

It is important to note that electrons emitted from a solid converter into gas experience energy-dependent scattering processes, and possible loss due to backscattering into the converter [Fig. 1, (1)]. The electron loss depends on the gas type and on the electric field at the converter surface; it is largest in noble gases and at small fields [20]. A field >1 kV/cm in atmospheric pressure is required to minimize the backscattering loss, which may cause inefficient electron focusing into the GEM holes. We extensively investigated the issue for semitransparent [21], [22]

Manuscript received October 29, 2003; revised July 14, 2004. This work was supported in part by the Israel Science Foundation and in part by the Planning and Budgeting Committee of the Council for Higher Education in Israel. The work of J. M. Maia and J. F. C. A. Veloso was supported by the Fundação para a Ciência e a Tecnologia, Lisbon, Portugal, under Project POCTI/FNU/49553/02 of the Instrumentation Centre (Unit 217/94), Physics Department, University of Coimbra. The work of V. Dangendorf and D. Mörmann was supported by the MINERVA foundation. The work of G. Guedes was supported by CAPES, Brazil.

R. Chechik, A. Breskin, and D. Mörmann are with the Weizmann Institute of Science, 76100 Rehovot, Israel (e-mail: Rachel.chechik@weizmann.ac.il).

G. P. Guedes was with the Weizmann Institute of Science, 76100 Rehovot, Israel, on leave from the Laboratory for Nuclear Instrumentation COPPE/UFRJ, Rio de Janeiro, Brazil. He is now with the Universidade Estadual de Feira de Santana, Feira de Santana-BA, 44030-460, Brazil.

J. M. Maia was with the Weizmann Institute of Science, 76100 Rehovot, Israel, on leave from the University of Coimbra and University of Beira-Interior, Portugal. He is now with the University of Coimbra and University of Beira-Interior, Portugal.

V. Dangendorf was with the Weizmann Institute of Science, 76100 Rehovot, Israel, on leave from PTB, Braunschweig, Germany. He is now with PTB, D-38116 Braunschweig, Germany.

D. Vartsky is with Soreq NRC, 81800 Yavne, Israel.

J. M. F. Dos Santos is with the University of Coimbra, Portugal.

J. F. C. A. Veloso is with the Physics Department, University of Aveiro, P-3810-193 Aveiro, Portugal, and with the Physics Department, University of Coimbra, P-3004-516 Coimbra, Portugal (e-mail: jveloso@gian.fis.uc.pt).

Digital Object Identifier 10.1109/TNS.2004.835628

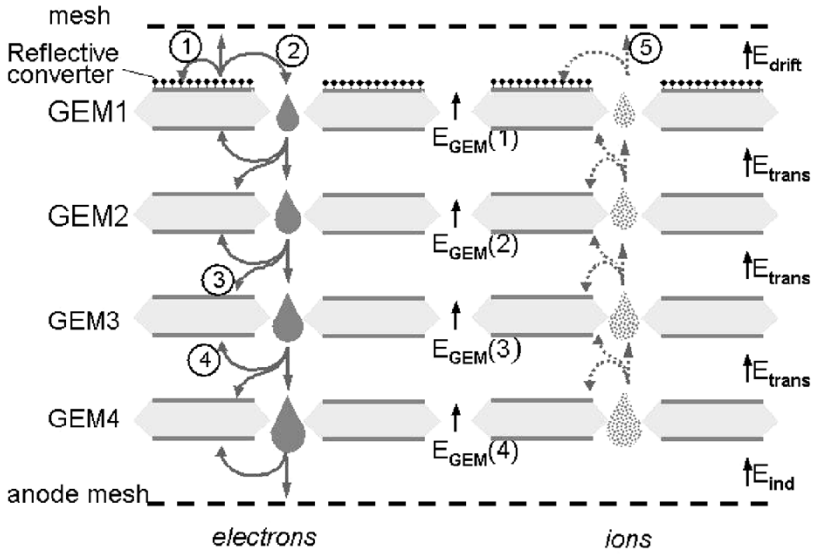

Fig. 1. Definition of notations and scheme of electron and ion transport processes in a 4-GEM detector with reflective solid converter.

and reflective [23], [24] operation modes. In the *semitransparent mode,* we confirmed that the highest possible ratio of the field $\mathrm{E_{GEM}}(1)$ (inside the GEM1 holes) to $\mathrm{E_{drift}}$ should be kept. The efficiency may not be 100% unless GEM1 gain is high, in the order of 10^3. In the *reflective mode* we showed that a sufficiently high field on the converter surface is established by high GEM1 voltage [23], [24]. We confirmed that fully efficient focusing [Fig. 1, (2)] and detection of the electrons is obtained when $\mathrm{E_{drift}} = 0$ and $\mathrm{E_{GEM}}(1)$ is high, corresponding to GEM1 gain of 10^2 to 10^3, depending on the gas [23], [24].

The transport of electrons between successive GEM electrodes may also be understood from Fig. 1: the extraction of electrons from the nth GEM toward its subsequent is expected to increase with the ratio $\mathrm{E_{trans}(n)/E_{GEM}}$, but their focusing into the holes of the next GEM decreases with the ratio $\mathrm{E_{trans}(n)/E_{GEM}(n)}$. The process has been comprehensively studied [19], confirming the expected trends. Preferable operation conditions are therefore based on a compromise, with a large fraction of the electron charge ($\sim$50%) lost on the GEM's faces [Fig. 1,(3) and (4)].

It is important to bear in mind that maintaining high transparency for the electrons implies similarly high transparency for avalanche ions flowing along the same field-lines in the opposite direction, with very little diffusion.

III. Ion Backflow

Backflowing avalanche ions may cause physical and chemical damage to the solid converter, and may affect its performance by charge accumulation on the surface. Furthermore, with converters of efficient secondary electron emission, secondary avalanches are initiated by the ions' impact *(ion feedback),* and this positive-feedback process severely limits the detector gain. Ions back flowing into the drift volume [Fig. 1, (5)] affect the operation of TPC devices as well [25]. The quantity named here *ion backflow* is the fraction of total avalanche-generated ions reaching the converter. Previous studies [19], [26]–[28] of this important quantity provided the general understanding of its dependence on the GEM geometry, gas type, pressure, fields, etc. It was demonstrated that the most effective parameter for ion backflow reduction is the field $\mathrm{E_{drift}}$. The ion backflow could also be blocked in the one-before-last GEM (e.g., using smaller holes, single-conical holes, smaller GEM voltage) [29], and the gain loss compensated by higher gain on the last GEM. But this asymmetric operation mode involves instability at high GEM voltages.

With *gas converters* $\mathrm{E_{drift}}$ can be kept small, thus limiting the ion backflow to the few percent level. However, with *solid converters,* in order to minimize electron backscattering, the field at the converter surface should always be kept high, and therefore the ions are strongly attracted to it. We have recently studied the ion backflow in a 4-GEM gaseous photomultiplier (with four identical GEM electrodes) with a *reflective CsI photocathode* [30]. As is obvious from Fig. 1, the ion extraction and transport follow trends similar to the electrons: ion transmission from the nth GEM upwards increases with the ratio $\mathrm{E_{trans}}(n-1)/\mathrm{E_{GEM}}(n)$, but their focusing into the holes of GEM$(n-1)$ decreases with the ratio $\mathrm{E_{trans}}(n-1)/\mathrm{E_{GEM}}(n-1)$. By varying all possible fields in the 4-GEM detector, but without sacrificing full photoelectron extraction and detection efficiency (namely keeping a high surface field on GEM1 and total gain of 10^6), we showed that the ion backflow may be reduced at best to $\sim$20% (Fig. 2). Operating the device with asymmetric powering of the last two GEMs may further reduce the ion backflow, by a few percent. We demonstrated an additional reduction of the ion backflow, to 10% (Fig. 2), by operating the induction gap (between the last GEM and the anode electrode) under high field $\mathrm{E_{ind}}$, in parallel-plate multiplication mode, with gain $>10^2$. In this case the final avalanche takes place at the induction volume where the majority of ions are produced and the high ratio $\mathrm{E_{ind}/E_{GEM}}(4)$ guarantees their inefficient focusing back into the last GEM. But with this approach

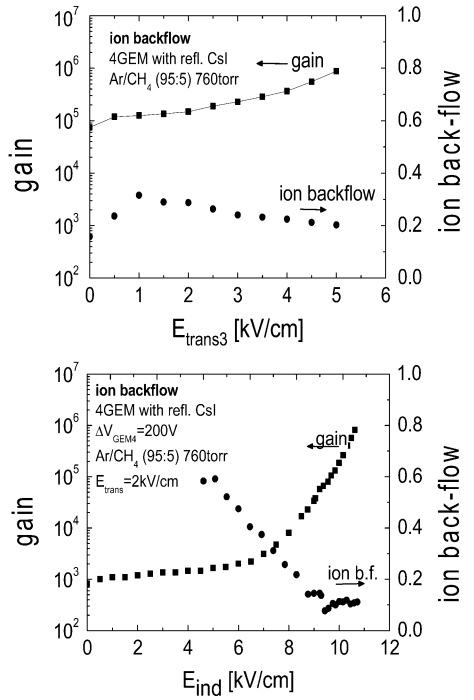

Fig. 2. Optimization of ion backflow in a 4-identical-GEMs detector, with reflective converter; on top the effect of the transfer field between GEM3 and GEM4 is shown, and at the bottom the effect of the induction field chosen in multiplication regime. The best ion backflow is 20% and 10% of the total charge gain, respectively.

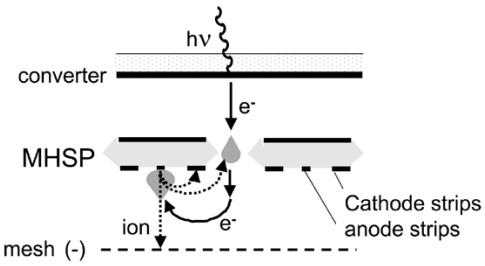

Fig. 3. The microhole and strip plate multiplier is a GEM-like device, etched with anode and cathode strips at its bottom. Two-stage electron multiplication occurs in the holes and further at the anode strips. Most of the final avalanche-ions may be collected at the nearby cathode strips and on the cathode mesh below.

the readout anode (Fig. 1) is no more decoupled from the multiplication electrodes, and there is a distinct ion component in the signal captured on the anode.

The MHSP electrode (Fig. 3) developed recently [17], [18] opens a way for further reduction of ion backflow. This GEM-like electrode has anode- and cathode- strips etched on its bottom face, and it operates in double-stage multiplication: the avalanche produced inside the hole is further multiplied on the anode strips. Consequently, a significant part of the ions are collected on adjacent cathode strips and, possibly, on the mesh or patterned readout electrode placed below the MHSP (Fig. 3). We have recently shown [31] that by replacing GEM4 in the detector of Fig. 1 with a MHSP electrode, new operating conditions could be used: the last mesh acts as a cathode, the charge flow is partially blocked by small $\mathrm{E_{trans}}(3)$, and the gain-loss is compensated by the anode-strips' multiplication.

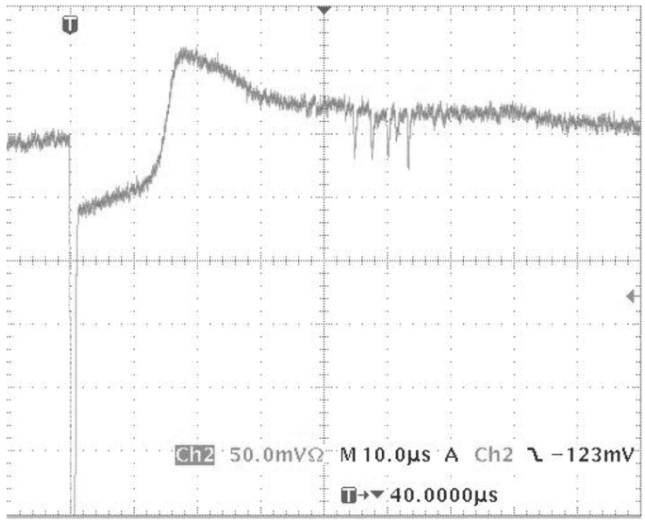

Fig. 4. Fast pulses recorded from the gated 4-GEM detector, with gate open. Starting at 45 μs after the main avalanche, corresponding to the ion drift-time to the converter, ion-induced secondary avalanches are seen.

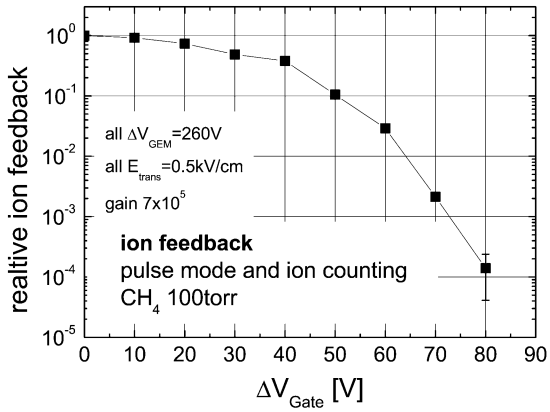

Fig. 5. Relative ion feedback obtained from ion-induced feedback avalanches counting (Fig. 4), as function of gate-pulse voltage. Suppression by factor 10^4 is demonstrated here at low pressure with 80 V gate-pulse; identical performance was confirmed at atmospheric pressure with 150–200 V gate pulse.

Under such conditions we reduced the ion backflow, in Ar/CH_4 (95:5), to $\sim$2.5% at effective gains of 10^5–10^6.

To practically suppress the ion backflow we have introduced [30] an active pulsed-gate electrode, as suggested in [25]. It consists of a parallel-wires plane, uniformly biased in the *open state* and *alternately biased*, by a $\pm$ voltage pulse, in the *closed state*. We have confirmed full electron transmission in the *open state*. We incorporated the gate electrode between GEM3 and GEM4 in a 4-GEM detector with *reflective CsI photocathode*, and operated it at 100 torr CH_4 in order to deliberately enhance the ion-induced secondary effects from the photocathode. Using 80 V, 10 μs-long gate pulses, triggered by the anode electron signal, and counting the secondary ion-induced pulses (Fig. 4), we showed [30] that the gate reduces the ion backflow by a factor 10^4, as shown in Fig. 5. We confirmed identical gate operation at atmospheric pressure, with gate pulses of 150–200 V. The dramatic ion backflow suppression is of course achieved at the expense of counting rate capability, due to the $\sim$10 μs dead time, which could be reduced by optimizing the detector's geometry.

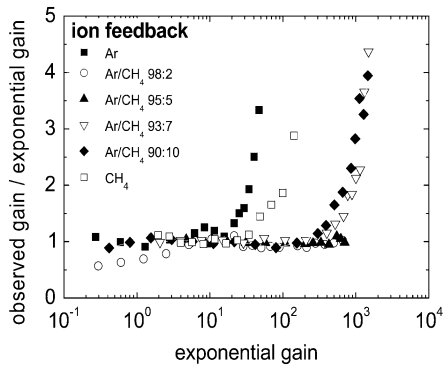

Fig. 6. Deviation of the recorded gain from the exponentially fitted one, as function of the last, measured in current mode with a single-GEM and semitransparent K-Cs-Sb photocathode, in various gas mixtures. The deviation, which occurs at different gains in different gases, is due to intensive secondary avalanches, shown in Fig. 7.

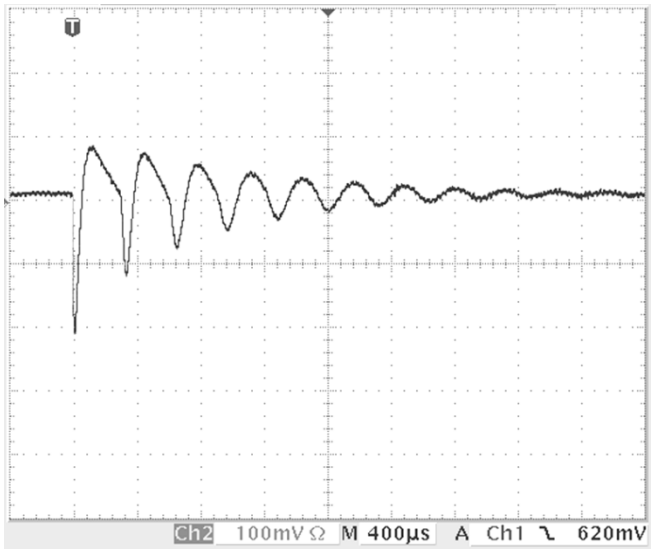

Fig. 7. Ion-induced feedback pulses, observed with a semitransparent K-Cs-Sb photocathode and a single GEM, operated with pure argon at gain >40.

We clearly demonstrated the need for such efficient suppression of ion backflow, in a multi-GEM photon detector with semitransparent K-Cs-Sb photocathode of visible-light range sensitivity. For this photocathode we measured the secondary electron emission probability under impact of back-flowing ions in Ar/CH_4 mixtures, to be 0.05 to 0.5 electrons/ion. The higher probability was recorded in pure Ar. Without ion gating, we found that secondary avalanches induced by impact of ions from the first GEM, limit its gain (Figs. 6 and 7); the gain limit varies from 30 to 1000, depending on the CH_4 percentage in the mixture. This dependence is derived mainly from the differences in electron backscattering and in ion backflow. The present interpretation, based on our recent systematic measurements, replaces our previous one given in [8].

IV. Timing and Localization

The use of solid radiation converters coupled to gaseous electron multipliers results in improved timing and localization properties [32]. Surface-emitted electrons undergo almost-synchronous fast multiplication within the GEM holes; the small gaps between consecutive GEMs' limit diffusion-governed avalanche spread, resulting in very fast pulses and good time resolution [4]. For example, in a 4-GEM detector operated in CF_4 with a reflective CsI photocathode, we recorded time resolutions of $\sigma = 0.33$ and 1.6 ns, with 150 and single photoelectrons, respectively. The point-like conversion and the small electron diffusion also result in excellent localization resolution while the granularity of the first GEM-electrode is expected to contribute typically less than 30 μm root mean square (rms) to the localization precision; the final avalanche lateral size is of the order of the hole diameter.

Multi-GEM detectors currently demonstrate localization resolutions of a few tens of μm rms with charged particles and soft X-rays; these are obtained with costly highly integrated readout electronics [7]. A different challenge in radiation imaging with large-area GEM-based detectors is to find more economic readout methods. For that purpose the initial, spatially narrow, charge induced on the readout electrode should be broadened, either by introducing a wide induction gap (between the last GEM and the readout anode) [33], or by recording induced charges behind a resistive charge-collection anode [34]. The latter efficiently broadens the charge distribution according to the distance between the resistive layer and the readout electrode, which is capacitively coupled and conveniently grounded. We investigated both techniques and applied them to the imaging of UV light, soft X-rays, and fast neutrons, as discussed below.

V. Applications of Cascaded-GEM Detectors

A. Detectors of Visible Light

Photon detectors with semitransparent K-Cs-Sb photocathode and four standard Kapton GEMs are currently sealed in packages filled with atmospheric Ar/CH_4 (95:5). The deposition and sealing system and processes, which were developed at our laboratory, as well as detector details, are described in [8]. So far, sealed detectors of that type had quantum efficiency above 6% at 360 nm and a photocathode lifetime of the order of one month, limited by sealing imperfection [8]. The latest version of this device includes a gate electrode, to suppress ion-feedback. Despite the apparent compatibility of Kapton GEMs, at least in the short term, efforts are being made to produce GEM electrodes of ultrahigh vacuum compatible materials such as ceramic and silicon [35]. Other candidate electron multipliers could be cascaded micro channel plate (MCP)-like glass-capillary multipliers [36].

B. UV-Photon Detectors

Among the important advantages of a reflective photocathode deposited on the first GEM (Fig. 1) is its operation with $E_{drift} = 0$, which renders the detector insensitive to ionizing background radiation crossing the drift volume. We have proposed [24] using such reflective-CsI photon detectors for the imaging of UV photons in ring imaging Cherenkov (RICH) devices, where high-multiplicity ionizing radiation is a principal limiting factor. We demonstrated the operation in

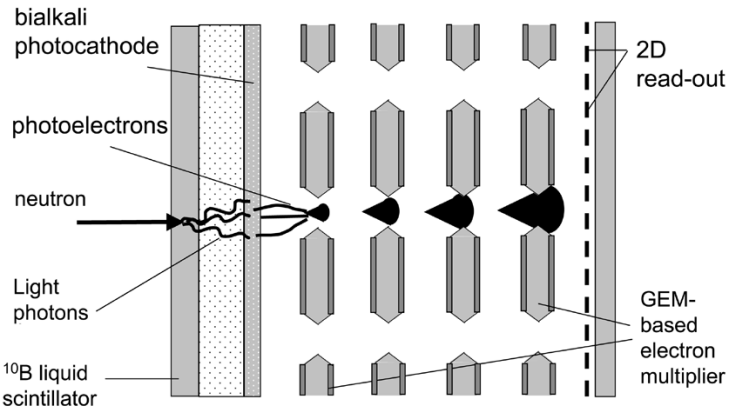

Fig. 8. A scheme of the novel thermal-neutron detector currently under development; it is based on boron-rich liquid scintillating converter coupled to a sealed multi-GEM photon detector. The thin scintillator, the efficient light coupling and the fast photoelectron multiplication in the GEM-based multiplier, guarantee fast response, low sensitivity to gamma background and very high neutron detection efficiency.

pure CF_4 [5], which permits conceiving windowless detectors with the radiator and the photon-detector operating within the same gas volume. Detectors based on this principle are currently being investigated for a Hadron-blind Cherenkov detector for the PHENIX experiment at relativistic heavy ion collider (RHIC) [37].

Based on the possibility of operating GEM- and GEM/MHSP-cascades in noble gas mixtures [4], we foresee their application in gas scintillation proportional chambers, with the scintillation volume directly coupled to the UV detector, within the same gas volume. Stable operation, with high gain and good energy resolution, was presented recently with a single MHSP element in atmospheric Ar/Xe (5%) mixture [38]. Xe-operated multi-GEM UV-detectors with CsI photocathodes were recently proposed by the XENON collaboration for recording scintillation light from liquid-Xe WIMP detectors [39]. Recent results on the operation of cascaded GEMs in such two-phase (liquid-gas) cryogenic detectors are given in [40].

C. X-Ray Imaging Detectors

We have developed a three-GEM X-ray imaging detector, where X-rays are converted in a gas gap. It has a 400-μm pitch striped X-Y anode-readout plane, coupled to fast (2.1 ns/tap) discrete-element delay lines [12]. Having a broad induction-gap we could match the lateral charge-distribution width, in Ar/CO_2 (70:30) and in Ar/CH_4 (95:5), to the anode pitch. The induced-pulse time-width was matched to the frequency transmission-characteristics of the line, with $<$20% signal attenuation along 100 mm [33], [12]. Despite the X-ray conversion in gas, we demonstrated intrinsic localization resolutions of $\sigma \sim 70$ μm. This simple and fast delay-line based readout scheme permits photon-counting imaging at 100 kHz.

The resistive electrode approach was recently investigated with cascaded GEM and GEM/MHSP multipliers, coupled to a wedge-and-strip (W&S) [41] readout electrode, of 1.6 mm pitch. Localization resolution of $\sigma = 60$ μm was recorded with 6 keV X-rays and a three-GEM multiplier; a resolution of $\sigma = 100$ μm was recorded with single UV photons, and a four-GEM multiplier coupled to a CsI photocathode. In both cases the W&S electrode was placed behind a resistive anode. In a two-GEM/MHSP detector the ion-induced signals were recorded at the W&S electrode placed behind a resistive cathode; a resolution of $\sigma = 100$ μm was obtained with 6 keV X-rays. More details are given in [38].

We foresee the development of high-resolution cascaded multi-GEM secondary electron emission (SEE) imaging detectors [32] with CsI-coated X-ray converters.

D. Thermal Neutron Imaging

We are currently developing a fast novel thermal-neutron imaging-detector [42], schematically depicted in Fig. 8. It comprises a thin ($<$0.5 mm)^{10} B-rich (22% boron content by weight) liquid-scintillator, with emission peaked at 350 nm, matched to the quantum efficiency of the photon detector described above (Section V-A). The detector is designed to have 0.95 efficiency to thermal neutrons (of 1.8 Å) and only 3×10^{-3} efficiency to γ. With pulse-shape discrimination procedure these efficiencies become 0.8 and 2×10^{-5}, respectively. The position resolution obtained with a fiber faceplate window is $\sim$500 μm and the time resolution (determined by the liquid converter thickness) is $\sim$200 ns.

E. Fast-Neutron Imaging

We have recently developed a novel fast-neutron imaging detector, depicted schematically in Fig. 9. The detector prototype (10 cm $\times$ 10 cm) comprises a 1 mm thick polyethylene converter coupled, via 1 mm thick gas converter, to a three-GEM detector. Protons originating from neutron conversion in the foil are converted in the gas and imaged with the multi-GEM detector. We implemented the resistive layer approach discussed above, and delay-line readout [43]. The readout-electrode has nonoverlapping X-Y pads of 2mm pitch, at the back side of a resistive layer anode; the pads are coupled to a fast delay-line (2.7 ns/tap). We showed that a resistive layer with surface resistivity $>$30 M$\Omega/\square$ (e.g., $\sim$160 nm Ge evaporated on glass or on 3.2 mm G-10) has $\sim$94% signal transmission. We recently demonstrated fast-neutron imaging capability with localization resolution $<$1 mm rms. Fig. 10 shows a radiographic image of carbon cylindrical phantoms and a metal wrench (the

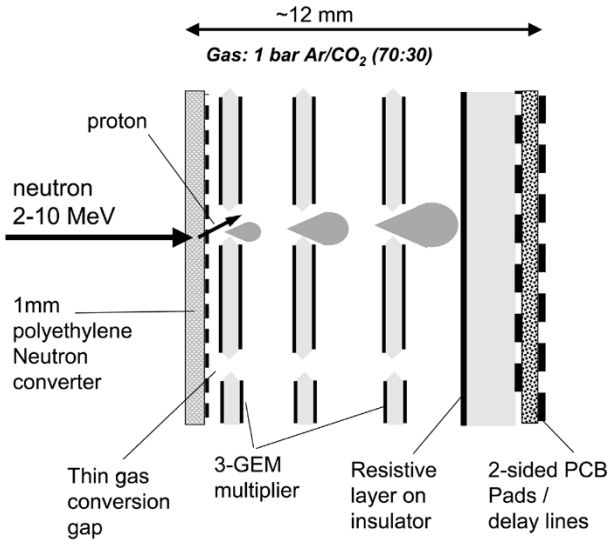

Fig. 9. Schematic view of the fast-neutron detector: 2 to 10 MeV neutrons are converted in polyethylene and the resulting protons are detected and imaged with a three-GEM detector; spatially broadened charge signals are recorded behind the resistive layer, on X-Y anode pads connected to delay-line readout.

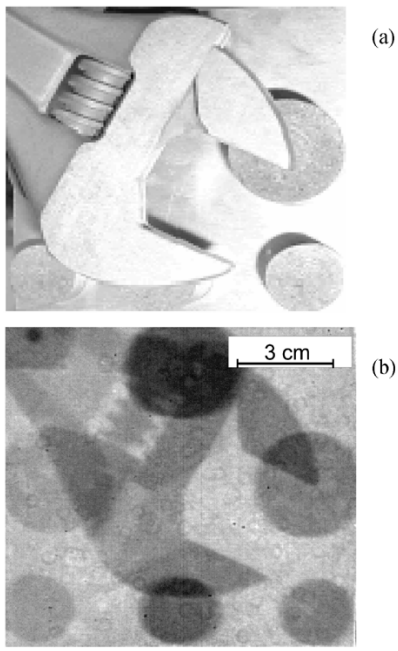

Fig. 10. A radiographic image (b) of the phantom (a) comprising 6 carbon cylinders and a metal wrench, recorded with a broad-energy neutron beam (3–10 MeV) and the novel fast-neutron detector.

wrench's screw is clearly visible at the center of the field view), recorded with a broad-energy neutron beam (3 to 10 MeV) and small statistics. The efficiency of the detector to MeV neutrons is $\sim$0.2%. To achieve higher efficiencies, for practical application in fast neutron radiography, we plan to combine 25 identical detector-layers in sequence, to obtain $\sim$5% efficiency. In a recent experiment, with a pulsed fast-neutron beam, a time resolution of $\sigma = 1.7$ ns was obtained.

VI. Summary

We have extensively studied the properties of multi-GEM detectors, particularly the processes involved in electron and ion transport and the key parameters controlling them. We have shown that with solid converters (semitransparent or reflective) ion backflow cannot be safely reduced below 15% to 20% of the total charge without affecting the electron transport, namely, losing quantum efficiency or gain. With the new MHSP multiplier replacing the last GEM in the cascade, ion backflow could be reduced to 2%. We demonstrated that a pulsed gating-electrode introduced in the cascade could effectively suppress ion backflow (and the resulting ion-induced feedback) by a factor of 10^4, without losing detection efficiency, although with introduction of some dead time.

We are applying multi-GEM detectors for the fast and efficient imaging of soft X-rays, fast- and thermal- neutrons, and UV-to-visible photons. Some examples were briefly presented, with concise discussion of readout methods, as well as localization and timing properties.

References

[1] F. Sauli, "GEM: A new concept for electron amplification in gas detectors," *Nucl. Instrum. Meth.*, vol. A386, pp. 531–534, 1997.
[2] ——, "Development and applications of gas electron multiplier detectors," *Nucl. Instrum. Meth.*, vol. A505, pp. 195–198, 2003.
[3] J. Benlloch *et al.*, "Further developments and beam tests of the gas electron multiplier (GEM)," *Nucl. Instrum. Meth.*, vol. A419, pp. 410–417, 1998.
[4] A. Buzulutskov, A. Breskin, G. Garty, R. Chechik, F. Sauli, and L. Shekhtman, "The GEM photomultiplier operated with noble gas mixtures," *Nucl. Instrum. Meth.*, vol. A 443, p. 164, 2000. "Further studies of the GEM photomultiplier," *Nucl. Instrum. Meth.*, vol. A442, pp. 68–73, 2000.
[5] A. Breskin, A. Buzulutskov, and R. Chechik, "GEM photomultiplier operation in CF_4," *Nucl. Instrum. Meth.*, vol. A483, pp. 670–675, 2002.
[6] A. Bressan, J. C. Labbé, P. Pagano, L. Ropelewski, and F. Sauli, "Beam tests of the gas electron multiplier," *Nucl. Instrum. Meth.*, pp. 262–276, 1999.
[7] S. Bachmann, S. Kappler, B. Ketzer, Th. Müller, L. Ropelewski, F. Sauli, and E. Schulte, "High rate x-ray imaging using multi-GEM detectors with a novel readout design," *Nucl. Instrum. Meth.*, vol. A478, pp. 104–108, 2002.
[8] M. Balcerzyk *et al.*, "Methods of preparation and performance of sealed gas photomultipliers for visible light," *IEEE Trans. Nucl. Sci.*, vol. 50, pp. 847–854, 2003.
[9] C. Altunbas *et al.*, "Construction, test and commissioning of the triple-GEM tracking detector for compass," *Nucl. Instrum. Meth.*, vol. A490, pp. 177–203, 2002.
[10] T. Behnke, S. Bertolucci, R. D. Heuer, and R. Settles, Eds., "A Detector for TESLA,", pt. IV, TESLA Tech. Design Rep., Mar. 2001.
[11] A. Bressan, R. De Oliveira, A. Gandi, J.-C. Labbé, L. Ropelewski, F. Sauli, D. Mörmann, T. Mûler, and H. J. Simonis, "Two-dimensional readout of GEM detectors," *Nucl. Instrum. Meth.*, vol. A425, pp. 254–261, 1999.
[12] G. P. Guedes *et al.*, "Two-dimensional GEM imaging detector with delay-line readout," *Nucl. Instrum. Meth.*, vol. A513, pp. 473–483, 2003.
[13] F. A. F. Fraga *et al.*, "CCD readout of GEM-based neutron detectors," *Nucl. Instrum. Meth.*, vol. A478, pp. 357–361, 2002.
[14] M. Klein, H. Abele, D. Fiolka, and Ch. Schmidt *et al.*, "A New efficient and position-sensitive detector for thermal neutrons on large areas," in *Art and Symmetry in Experimental Physics*, D. Budker *et al.*, Eds. Melville, NY: American Institute of Physics, 2001.
[15] R. Chechik *et al.*, "Progress in GEM-based gaseous photomultipliers," *Nucl. Instrum. Meth.*, vol. A502, pp. 195–199, 2003.
[16] D. Mörmann, M. Balcerzyk, A. Breskin, R. Chechik, B. K. Singh, and A. Buzulutskov, "GEM-based gaseous photomultipliers for UV and visible photon imaging," *Nucl. Instrum. Meth.*, vol. A504, pp. 93–98, 2003.

[17] J. F. C. A. Veloso, J. M. F. dos Santos, and C. A. N. Conde, "A proposed new microstructure for gas radiation detectors: The microhole and strip plate," *Rev. Sci. Instrum.*, vol. 71, pp. 2371–2376, 2000.

[18] J. M. Maia, J. F. C. A. Veloso, J. M. F. dos Santos, A. Breskin, R. Chechik, and D. Mörmann, "Advances in the micro-hole & strip plate gaseous detector," *Nucl. Instrum. Meth.*, vol. A504, pp. 364–368, 2003.

[19] S. Bachmann, A. Bressan, L. Ropelewski, F. Sauli, A. Sharma, and D. Mörmann, "Charge amplification and transfer processes in the gas electron multiplier," *Nucl. Instrum. Meth.*, vol. A438, pp. 376–408, 1999.

[20] A. Di Mauro *et al.*, "Photoelectron backscattering effects in photoemission from CsI into gas media," *Nucl. Instrum. Meth.*, vol. A371, pp. 137–142, 1996.

[21] C. Richter, A. Breskin, R. Chechik, D. Mörmann, G. Garty, and A. Sharma, "On the efficient electron transfer through GEM," *Nucl. Instrum. Meth.*, vol. A478, pp. 538–558, 2002.

[22] A. Sharma, "Detection of single electrons with a GEM," *Nucl. Instrum. Meth.*, vol. A471, pp. 136–139, 2001.

[23] D. Mörmann, A. Breskin, R. Chechik, and B. K. Singh, "On the efficient operation of a CsI-coated GEM photon detector," *Nucl. Instrum. Meth.*, vol. A471, pp. 333–339, 2001.

[24] D. Mörmann, A. Breskin, R. Chechik, P. Cwetanski, and B. K. Singh, "A gas avalanche photomultiplier with a CsI-coated GEM," *Nucl. Instrum. Meth.*, vol. A478, pp. 230–234, 2002.

[25] P. Némethy, P. J. Oddone, N. Toge, and A. Ishibashi, "Gated time projection chambers," *Nucl. Instrum. Meth.*, vol. 212, pp. 273–280, 1983.

[26] A. Breskin, A. Buzulutskov, R. Chechik, B. K. Singh, A. Bondar, and L. Shekhtman, "Sealed GEM photomultiplier with a CSI photocathode: Ion feedback and ageing," *Nucl. Instrum. Meth.*, vol. A478, p. 225, 2002.

[27] A. Buzulutskov, "Physics of multi-GEM structures," *Nucl. Instrum. Meth.*, vol. A494, pp. 148–155, 2002.

[28] F. Sauli, S. Kappler, and L. Ropelewski, "Electron collection and ion feedback in GEM-based detectors," *IEEE Trans. Nucl. Sci.*, vol. 50, pp. 803–808, 2003.

[29] A. Bondar, A. Buzulutskov, L. Shekhtman, and A. Vasiljev, "Study of ion feedback in multi-GEM structures," *Nucl. Instrum. Meth.*, vol. A496, pp. 325–332, 2003.

[30] D. Mörmann, A. Breskin, R. Chechik, and D. Bloch, "Evaluation and reduction of ion back-flow in multi-GEM detectors," *Nucl. Instrum. Meth.*, vol. A516, pp. 315–326, 2004.

[31] J. M. Maia, D. Mörmann, A. Breskin, R. Chechik, J. F. C. A. Veloso, and J. M. F. dos Santos, "Avalanche-ion back-flow reduction in gaseous electron multipliers based on GEM/MHSP," *Nucl. Instrum. Meth.*, to be published.

[32] A. Breskin, "Secondary emission gaseous detectors: a new class of radiation imaging detectors," *Nucl. Phys. B (Proc. Suppl.)*, vol. 44, pp. 351–363, 1995.

[33] G. Guedes, A. Breskin, R. Chechik, and D. Mörmann, "Effects of the induction-gap parameters on the signal in a double-GEM detector," *Nucl. Instrum. Meth.*, vol. A497, pp. 305–313, 2003.

[34] O. Jagutzki, J. S. Lapington, L. B. C. Worth, U. Spillman, V. Mergel, and H. Schmidt-Böcking, "Position sensitive anodes for MCP read-out using induced charge measurement," *Nucl. Instrum. Meth.*, vol. A477, pp. 256–261, 2002.

[35] A. Breskin, M. Balcerzyk, R. Chechik, G. P. Guedes, J. Maia, and D. Mörmann, "Recent advances in gaseous imaging photomultipliers," *Nucl. Instrum. Meth.*, vol. A513, pp. 250–255, 2003.

[36] V. Biteman, S. Guinji, V. Peskov, H. Sakurai, E. Silin, T. Sokolova, and I. Radionov, "Position sensitive gaseous photomultipliers," *Nucl. Instrum. Meth.*, vol. A471, pp. 205–208, 2001. references therein.

[37] A. Koslov, I. Ravinovitch, L. Shekhtman, Z. Fraenkel, M. Inuzuka, and I. Tserruya, "Development of a triple GEM UV-photon detector operated in pure CF_4 for the PHENIX experiment," *Nucl. Instrum. Meth. A*, to be published.

[38] J. M. Maia, D. Mörmann, A. Breskin, R. Chechik, J. F. C. A. Veloso, and J. M. F. dos Santos, "Progress in MHSP multiplier operation," *IEEE Trans. Nucl. Sci.*, vol. 51, pp. 1503–1508, June 2004.

[39] E. Aprile *et al.*, The XENON Project. astro-ph/0 207 670.

[40] A. Buzulutskov, A. Bondar, L. Shekhtman, R. Snopkov, and Y. Tikhonov, "First results from cryogenic avalanche detectors based on gas electron multipliers," *IEEE Trans. Nucl. Sci.*, vol. 50, pp. 2491–2494, 2003.

[41] O. H. W. Siegmund, S. Clothier, J. Thornton, J. Lemen, R. Harper, I. M. Mason, and J. L. Culhane, "Application of the wedge and strip anode to position sensing with microchannel plates and proportional counters," *IEEE Trans. Nucl. Sci.*, vol. 30, pp. 503–507, 1983.

[42] D. Vartsky, M. B. Goldberg, A. Breskin, R. Chechik, B. Guerard, and J. F. Clergeau, "Large area imagine detector for neutron scattering based on Boron-rich liquid scintillator," *Nucl. Instrum. Meth.*, vol. A 504, pp. 369–373, 2003.

[43] V. Dangendorf, A. Breskin, R. Chechik, C. Kersten, G. Laczko, O. Jagutzky, and D. Vartzky, "Novel detectors for time-of-flight fast-neutron radioscopy," *Nucl. Instrum. Meth. A*, to be published.